Supplementary Information Titles

Journal: Nature Medicine

Article Title:	Interleukin-33-induced expression of progesterone-induced blocking factor 1 by decidual B cells protects against preterm labor
Corresponding Author:	Kang Chen

Supplementary Item & Number	**Title or Caption**
Supplementary Table 1	Demographic and clinical characteristics of the study subjects.
Supplementary Table 2	qRT-PCR primers used in this study.
Supplementary Table 3	Antibodies used in this study.
Supplementary Figure 1	B cells are present in choriodecidua of women undergoing TL or PTL at delivery.
Supplementary Figure 2	Human choriodecidua harbors B cells with increased activation, class switching and plasmacytoid differentiation compared to peripheral blood B cells.
Supplementary Figure 3	Human PTL choriodecidua expresses increased B cell-stimulating factors.
Supplementary Figure 4	B cell deficiency in mice causes heightened uterine inflammation and higher uterine neutrophil, but not inflammatory monocyte, infiltration and activation following LPS administration in late gestation.
Supplementary Figure 5	B cells mediate protection against LPS-induced PTL in mice independently of IL-10, TGF-β or IL-35.
Supplementary Figure 6	Human choriodecidual B cells express PIBF1 at term delivery.
Supplementary Figure 7	B cells are a significant producer of PIBF1 in mouse uterus during late pregnancy.
Supplementary Figure 8	B cells are a significant producer of PIBF1 in human choriodecidua at term delivery.
Supplementary Figure 9	Full-length PIBF1 administration suppresses uterine inflammation and neutrophil activation in LPS-challenged pregnant μMT mice.
Supplementary Figure 10	A C-terminal fragment of PIBF1 does not protect μMT mice against LPS-induced PTL.
Supplementary Figure 11	IFN-γ, TNF, IL-17A, IL-4, IL-10, TGF-β, IL-25 and TSLP do not induce PIBF1 expression by human B cells.
Supplementary Figure 12	PIBF1 expression is diminished in uterine tissues and uterine B cells in *Il33*$^{-/-}$ mice.
Supplementary Figure 13	Mouse uterine PIBF1 expression does not reduce amidst systemic progesterone withdrawal in late gestation.
Supplementary Figure 14	Peripheral blood and choriodecidual B cells constitutively express IL1RAcP.
Supplementary Figure 15	Diminished ST2L expression on human PTL choriodecidual B cells was not due to lower choriodecidual progesterone.

Supplementary tables

Supplementary Table 1 Demographic and clinical characteristics of the study subjects♫

	Spontaneous TL (*n* = 30)	**Spontaneous PTL (*n* = 15)**	***P***
Maternal age (year) Median [interquartile range]	27.5 [24.75 – 29]	24 [23 – 28]	0.202‡
Race			0.564#
African-American	17 (56.6)	10 (66.7)	
White	9 (30)	3 (20)	
Hispanic	2 (6.7)	2 (13.3)	
Other	2 (6.7)	0 (0)	
Gestational length (week) Median [interquartile range]	39 [38 – 40]	34 [33 – 35]	< 0.0001$

♫: Subjects with current diagnosis of preeclampsia, a prior history or current diagnosis of diabetes, chronic hypertension, asthma, thyroid disease, pyelonephritis, active Chlamydia, Gonorrhea or Syphilis infections, active human papillomavirus (HPV) or herpes simplex virus (HSV) lesions, human immunodeficiency virus (HIV) infection and recreational drug use were excluded.
‡: 2-tailed *t*-test.
$: Kruskal–Wallis test.
#: 2-tailed Chi-square test.

Nature Medicine: doi:10.1038/nm.4244

Supplementary Table 2 qRT-PCR primers used in this study

Target gene		Primer sequence
Human		
GAPDH	S	5′– GAAGGTGAAGGTCGGAGTC –3′
	AS	5′– GAAGATGGTGATGGGATTTC –3′
PIBF1	S	5′– CTTACAAAGATTGAAGAATTGGAGG –3′
	AS	5′– AATTCTTGATATTTGCTGGCATCTT –3′
TNFSF13	S	5′– CTGCACCTGGTTCCCATTAAC –3′
	AS	5′– AAGAGCTGGTTGCCACATCAC –3′
TNFSF13B	S	5′– ACCGCGGGACTGAAAATCT –3′
	AS	5′– CACGCTTATTTCTGCTGTTCTGA –3′
TSLP	S	5′– CCCAGGCTATTCGGAAACTCAG –3′
	AS	5′– CGCCACAATCCTTGTAATTGTG –3′
Mouse		
Gapdh	S	5’ – AGGTCGGTGTGAACGGATTTG –3′
	AS	5’ – TGTAGACCATGTAGTTGAGGTCA –3′
Tnf	S	5’ – GGAACACGTCGTGGGATAATG –3′
	AS	5’ – GGCAGACTTTGGATGCTTCTT –3’
Il1b	S	5’ – GCAACTGTTCCTGAACTCAACT –3’
	AS	5’ – ATCTTTTGGGGTCCGTCAACT –3’
Il6	S	5’ – TAGTCCTTCCTACCCCAATTTCC –3’
	AS	5’ – TTGGTCCTTAGCCACTCCTTC –3’
Mmp9	S	5’ – GGACCCGAAGCGGACATTG –3’
	AS	5’ – CGTCGTCGAAATGGGCATCT –3’
Cxcl1	S	5’ – CTGGGATTCACCTCAAGAACATC –3’
	AS	5’ – CAGGGTCAAGGCAAGCCTC –3’
Cxcl5	S	5’ – GCGGCTATGACTGAGGAAGG –3’
	AS	5’ – GTTCCATCTCGCCATTCATGC –3’
Pibf1	S	5’ – GCTGACAGAAGAGCAGTATG –3’
	AS	5’ – CGAGCTCATAGAAGCGAATAG –3’
Cxcl2	S	5’ – CCAACCACCAGGCTACAGG –3’
	AS	5’ – GCGTCACACTCAAGCTCTG –3’
Ccl3	S	5’ – TTCTCTGTACCATGACACTCTGC –3’
	AS	5’ – CGTGGAATCTTCCGGCTGTAG –3’

Nature Medicine: doi:10.1038/nm.4244

Cxcl10	S	5’ – CCAAGTGCTGCCGTCATTTTC –3’
	AS	5’ – GGCTCGCAGGGATGATTTCAA –3’
Ccl2	S	5’ – TTAAAAACCTGGATCGGAACCAA –3’
	AS	5’ – GCATTAGCTTCAGATTTACGGGT –3’
Cxcl9	S	5’ – TCCTTTTGGGCATCATCTTCC –3’
	AS	5’ – TTTGTAGTGGATCGTGCCTCG –3’
Ebi3	S	5’ – CTCTCCCCTGGTTACACTG –3’
	AS	5’ – CCACGGGATACCGAGAAGC –3’
Il10	S	5’ – GCTCTTACTGACTGGCATGAG –3’
	AS	5’ – CGCAGCTCTAGGAGCATGTG –3’
Tgfb1	S	5’ – CTTCAATACGTCAGACATTCGGG –3’
	AS	5’ – GTAACGCCAGGAATTGTTGCTA –3’

Nature Medicine: doi:10.1038/nm.4244

Supplementary Table 3 Antibodies used in this study

Antigen	Conjugation	Isotype	Clone	Manufacturer	Use
Human					
APRIL	–	Goat IgG	–	Santa Cruz sc-5737	IF
BAFF	PE	Mouse IgG1	1D6	eBioscience 12-9017	IF
BAFFR	PE	Mouse IgG1	11C1	Biolegend 316906	FC
BCMA	PE	Goat IgG	–	R&D FAB193P	FC
CCR10	APC	Rat IgG2a	314305	R&D FAB3478A	FC
CCR6	PE	Mouse IgG2b	G034E3	Biolegend 353409	FC
CCR7	PE-Cy7	Rat IgG2a	3D12	BD 557648	FC
CCR9	AF647	Mouse IgG2a	BL/CCR9	Biolegend 346301	FC
CD10	PE	Mouse IgG1	MEM-78	Thermo Fisher Scientific CD1004	FC
CD11c	PE	Mouse IgG1	B-ly6	BD 555392	FC
CD138	PE	Mouse IgG1	DL-101	BD 555805	FC
CD14	PerCP-Vio700	Mouse IgG2a	TÜK4	Miltenyi Biotec 130-097-539	FC
CD15	FITC	Mouse IgM	HI98	BD 555401	FC
CD16	APC-Cy7	Mouse IgG1	3G8	BD 557758	FC
CD19	APC-Cy7	Mouse IgG1	HIB19	Biolegend 302218	FC
	PE-Cy7	Mouse IgG1	HIB19	eBioscience 25-0199	FC
	Biotin	Mouse IgG1	HIB19	Biolegend 302204	MACS, IF, IHC
	PE-CF594	Mouse IgG1	HIB19	BD 562321	FC
	QDot655	Mouse IgG1	SJ25C1	Thermo Fisher Scientific Q10179	FC
CD1d	PE	Mouse IgG2b	51.1	Biolegend 350305	FC
CD20	PE-Cy7	Mouse IgG2b	2H7	Biolegend 302312	FC
	APC	Mouse IgG2b	2H7	Biolegend 302310	FC

Nature Medicine: doi:10.1038/nm.4244

CD22	PE	Mouse IgG2b	S-HCL-1	BD 347577	FC
CD23	FITC	Mouse IgG1	9P25	Beckman Coulter IM0529	FC
CD24	PE	Mouse IgG2a	ML5	BD 555428	FC
	APC-eF780	Mouse IgG1	eBioSN3	eBioscience 47-0247	FC
CD25	FITC	Mouse IgG1	M-A251	BD 555431	FC
CD27	AF647	Mouse IgG1	O323	Biolegend 302812	FC
	PE	Mouse IgG1	M-T271	BD 555441	FC
CD3	PerCP-Vio700	Mouse IgG2a	BW264/56	Miltenyi Biotec 130-100-458	FC
CD38	PE-Cy7	Mouse IgG1	HIT2	Biolegend 303510	FC
	APC	Mouse IgG1	HIT2	Biolegend 303516	FC
CD4	FITC	Mouse IgG1	RPA-T4	eBioscience 25-0049	FC
CD40	FITC	Mouse IgG1	5C3	Biolegend 334305	FC
CD43	FITC	Mouse IgG1	84-3C1	eBioscience 11-0439	FC
CD44	PE	Rat IgG2b	IM7	Biolegend 103009	FC
CD45	eF450	Mouse IgG1	2D1	eBioscience 48-9459	FC
CD5	PE	Mouse IgG1	UCHT2	BD 555353	FC
CD56	PE-Cy7	Mouse IgG2a	MEM 188	Biolegend 304628	FC
CD69	PE	Mouse IgG1	FN50	BD 555531	FC
CD70	PE	Mouse IgG1	113-16	Biolegend 355103	FC
CD8	PE	Mouse IgG1	RPA-T8	BD 555367	FC
CD80	PE	Mouse IgG1	L307.4	BD 557227	FC
CD86	PE	Mouse IgG1	FUN-1	BD 555658	FC
CD95	PE	Mouse IgG1	DX2	BD 555674	FC
Cytokeratin-7	–	Mouse IgG1	RCK105	Abcam ab9021	IF
GAPDH	–	Mouse IgG	–	Bioss bsm-0978M	WB

Nature Medicine: doi:10.1038/nm.4244

IgD	Biotin	Goat IgG F(ab)$_2$	–	Southern Biotech 2032-08	FC, MACS
	FITC	Mouse IgG2a	IA6-2	BD 555778	FC
IgM	FITC	Goat IgG F(ab)$_2$	–	Thermo Fisher Scientific AHI1608	FC
IL-10	PE	Rat IgG1	JES3-9D7	eBioscience 12-7108	FC
IL-17RB	AF488	Rabbit IgG	–	Bioss bs-2610R-FITC	FC
IL1RAcP	PE	Recombinant Human IgG	REA558	Miltenyi Biotec 130-108-756	FC
IL-33	–	Mouse IgG1	12B3C4	Thermo Fisher Scientific MA5-15772	WB
PD-L1	FITC	Mouse IgG1	MIH1	BD 558065	FC
PIBF1	–	Sheep IgG	–	R&D AF5559	WB, FC
	–	Rabbit IgG	–	Antibodies-online ABIN2426350	WB
ST2	–	Goat IgG	–	R&D AF523SP	WB
ST2L	FITC	Mouse IgG1	B4E6	MDBioproducts 101002F	FC
TACI	PE	Mouse IgG1	165604	R&D FAB1741P	FC
TSLP	–	Rabbit IgG	–	Rockland 600-401-FR6	IF
TSLPR	PE	Mouse IgG1	1B4	Biolegend 322806	FC
α_4 integrin	APC	Mouse IgG1	9F10	Biolegend 304308	FC
β_7 integrin	eF650NC	Rat IgG2a	FIB504	eBioscience 95-5867	FC
β-Actin	–	Mouse IgG1	AC-15	Sigma Aldrich A5441	WB
Mouse					
B220	APC-Cy7	Rat IgG2a	RA3-6B2	Biolegend 103224	FC
CD11b	APC-Cy7	Rat IgG2b	M1/70	Biolegend 101226	FC
CD11c	PE-Cy7	Hamster IgG	N418	Tonbo Biosciences 60-0114	FC
CD16/CD32	–	Rat IgG2b	2.4G2	Tonbo Biosciences 70-0161, BD Biosciences 553141	Fc Block
CD18	PerCP-Cy5.5	Rat IgG1	H155-78	Biolegend 141007	FC

Nature Medicine: doi:10.1038/nm.4244

CD19	PE-CF594	Rat IgG2a	1D3	BD 562291	FC
	BV650	Rat IgG2a	6D5	Biolegend 115541	FC
	FITC	Rat IgG2a	1D3	Tonbo Biosciences 35-0193	FC
CD3	APC-Cy7	Rat IgG2b	17A2	Tonbo Biosciences 25-0032	FC
CD44	PE-Cy7	Rat IgG2b	IM7	BD 560569	FC
CD45	violetFluor450	Rat IgG2b	30-F11	Tonbo Biosciences 75-0451	FC
CD62L	PE-Cy7	Rat IgG2a	MEL-14	Biolegend 104418	FC
CD86	AF700	Rat IgG2a	GL-1	Biolegend 105024	FC
CD95	PE	Hamster IgG2	Jo2	BD 554258	FC
F4/80	PE	Rat IgG2a	BM8	eBioscience 12-4801	FC
ICAM-1	Biotin	Rat IgG2b	YN1/1.7.4	Biolegend 116103	FC
IL-10	PE	Rat IgG2b	JES6-16E3	eBioscience 12-7101	FC
IL-33	–	Rabbit IgG	13H20L1	Thermo Fisher Scientific 700268	WB
iNOS	PE	Rat IgG2a	CXNFT	eBioscience 12-5920	FC
Ly-6C	PerCP-Cy5.5	Rat IgG2c	HK1.4	Biolegend 128012	FC
Ly-6G	FITC	Rat IgG2a	1A8	Tonbo Biosciences 35-1276	FC
MHC-II (I/A-I/E)	Biotin	Rat IgG2b	M5/114.15.2	Biolegend 107603	FC
NK1.1	PE-Cy7	Mouse IgG2a	PK136	Biolegend 108718	FC
	FITC	Mouse IgG2a	PK136	Biolegend 108714	FC
Pibf1	–	Sheep IgG	–	R&D AF5559	WB, FC
β-Actin	–	Mouse IgG1	AC-15	Sigma-Aldrich A5441	WB

Nature Medicine: doi:10.1038/nm.4244

Isotype controls	Conjugation	Clone	Manufacturer	Use
Goat IgG	–	–	Santa Cruz sc-2028	IF
	PE	Poly24030	Biolegend 403004	FC
Goat IgG F(ab')$_2$	Biotin	–	Southern Biotech 0110-08	FC
	FITC	–	Southern Biotech 0110-02	FC
Hamster IgG2	PE	B81-3	BD 550085	FC
Mouse IgG1	–	MOPC-21	BD 556648	IF
	AF647	MOPC-21	Biolegend 400155	FC
	APC	MOPC-21	BD 555751, Biolegend 400120	FC
	Biotin	MOPC-21	Biolegend 400103	FC, IHC
	FITC	MOPC-21	BD 555748	FC
	PE	MOPC-21	BD 555749	FC
	PE-Cy7	MOPC-21	BD 555872, Biolegend 400126	FC
Mouse IgG2a	AF647	MOPC-173	Biolegend 400234	FC
	FITC	X39	BD 349051	FC
	PE	MOPC-173	Biolegend 400212	FC
Mouse IgG2b	FITC	MPC-11	Biolegend 400310	FC
	APC	27-35	BD 555745	FC
	PE	eBMG2b	eBioscience 12-4732	FC
	PE-Cy7	MPC-11	Biolegend 400326	FC
	APC-eF780	eBMG2b	eBioscience 47-4732	FC
Rabbit IgG	–	–	Santa Cruz sc-2027	IF
	FITC	–	Bioss bs-0295P-FITC	FC
Rat IgG1	PE	eBRG1	eBioscience 12-4301	FC
	PerCP-Cy5.5	A110-1	BD 551072	FC

Nature Medicine: doi:10.1038/nm.4244

Rat IgG2a	AF700	RTK4530	Biolegend 400628	FC
	APC	RTK2758	Biolegend 400511	FC
	eF660	eBR2a	eBioscience 50-4321	FC
	FITC	R35-95	BD 554688	FC
	PE	eBR2a	eBioscience 12-4321	FC
	PE-Cy7	RTK2758	Biolegend 400521	FC
Rat IgG2b	Biotin	RTK4530	Biolegend 400603	FC
	PE	A95-1	BD 553989	FC
	PE-Cy7	RTK4530	Biolegend 400617	FC
Recombinant human IgG	PE	REA293	Miltenyi Biotec 130-104-613	FC
Sheep IgG	–	–	R&D 5-001-A	FC, IHC

Secondary antibody/reagent	**Conjugation**	**Manufacturer**	**Use**
Anti-biotin IgG	Magnetic microbeads	Miltenyi Biotec 130-090-485	MACS
Donkey anti-goat IgG	HRP	Santa Cruz sc-2020	WB
Donkey anti-mouse IgG	AF594	Thermo Fisher Scientific A21203	IF
	CF647	Sigma-Aldrich SAB4600176	IF
	HRP	Santa Cruz sc-2318	WB
Donkey anti-sheep IgG	HRP	Santa Cruz sc-2473	WB, IHC
Donkey F(ab')$_2$ anti-sheep IgG	AF647	Jackson Immunoresearch 713-606-147	IF
Goat F(ab')$_2$ anti-mouse IgG	Cy3	Jackson Immunoresearch 115-166-006	IF
	FITC	Southern Biotech 1032-02	IF
Goat F(ab')$_2$ anti-rabbit IgG	Cy3	Jackson Immunoresearch 111-166-047	IF
Goat anti-rabbit IgG	HRP	Santa Cruz sc-2004	WB

Nature Medicine: doi:10.1038/nm.4244

Streptavidin	AF488	Thermo Fisher Scientific S11223	FC, IF
	AF647	Thermo Fisher Scientific S21374	FC, IF
	ALP	Vector Laboratories SA-5100	IHC
	HRP	R&D 890803	IHC
	PerCP-Cy5.5	BD 551419	FC
	QDot605	Thermo Fisher Scientific Q10101MP	FC

Nature Medicine: doi:10.1038/nm.4244

Supplementary figures and legends

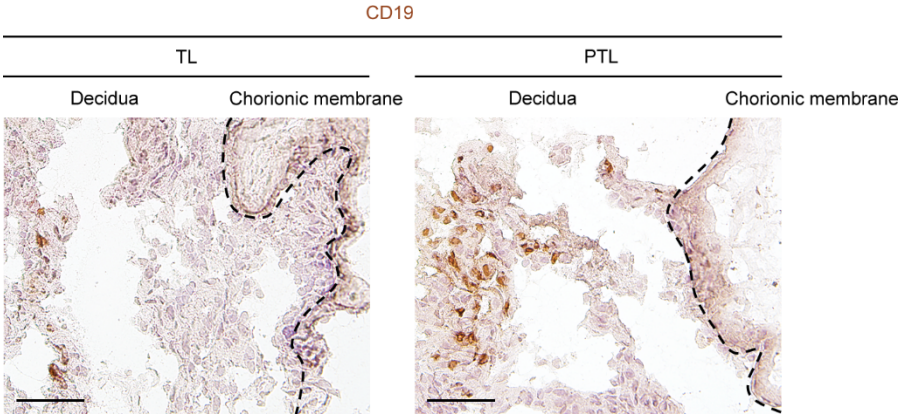

Supplementary Figure 1 B cells are present in choriodecidua of women undergoing TL or PTL at delivery. Immunohistochemical analysis of CD19 in the choriodecidual tissue of a woman undergoing TL (left) and a woman undergoing PTL (right). Nuclei were countered stained with hematoxylin. The dotted lines outline chorioamniotic membranes. Scale bars, 50 μm.

Nature Medicine: doi:10.1038/nm.4244

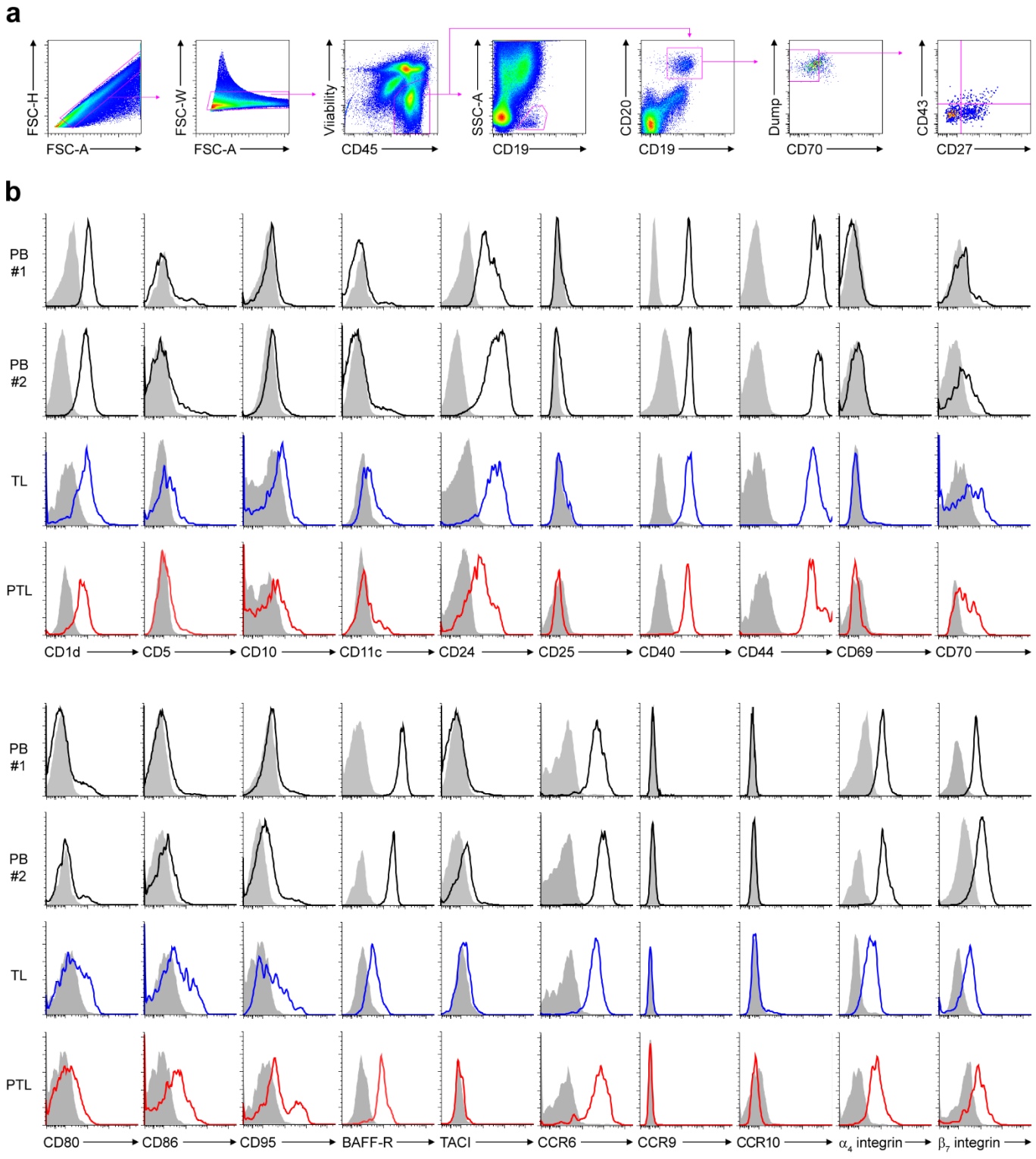

Supplementary Figure 2 Human choriodecidua harbors B cells with increased activation, class switching and plasmacytoid differentiation compared to peripheral blood B cells. (**a**) The flow cytometry gating strategy for the identification of choriodecidual $CD19^+$ B cells and $CD19^+CD20^+CD70^-CD27^+CD43^+$ cells. (**b**) The expression of CD1d, CD5, CD10, CD11c, CD24,

Nature Medicine: doi:10.1038/nm.4244

CD25, CD40, CD44, CD69, CD70, CD80, CD86, CD95, BAFF-R, TACI, CCR6, CCR9, CCR10, α_4 integrin and β_7 integrin on viable PB B cells (black histograms), choriodecidual B cells of women with TL (blue histograms) and PTL (red histograms). Shaded histograms indicate the fluorescence signals of the respective gated B cells generated by isotype-matched control antibodies. The results represent the staining profiles of 20 healthy blood donors, 16 women with TL and 12 women with PTL.

Nature Medicine: doi:10.1038/nm.4244

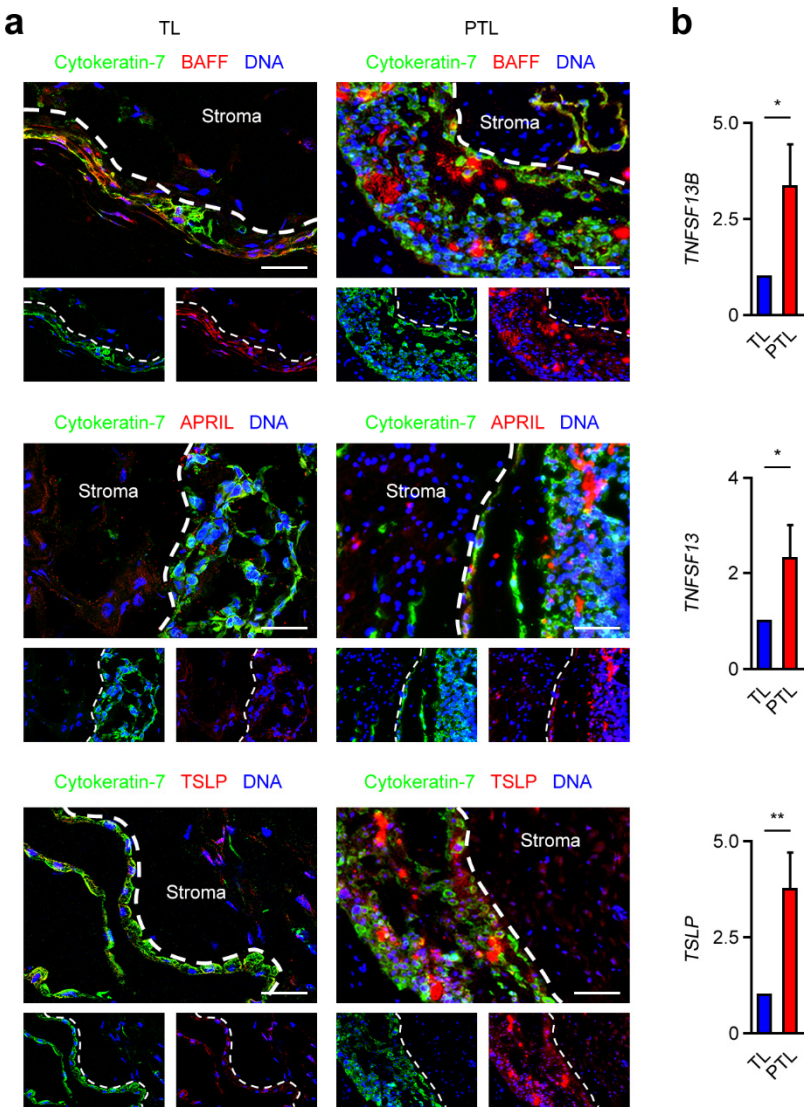

Supplementary Figure 3 Human PTL choriodecidua expresses increased B cell-stimulating factors. (**a**) Immunofluorescence analysis of choriodecidual tissues of a woman with TL and a woman with PTL for Cytokeratin-7 (green), BAFF, APRIL or TSLP (red) and DAPI-stained DNA (blue). Dotted lines mark the boundary between chorioamniotic epithelia and choriodecidual stroma. Scale bars, 50 μm. (**b**) Relative expression of *TNFSF13B* (BAFF), *TNFSF13* (APRIL) and *TSLP* transcripts in choriodecidual tissues of women with spontaneous TL ($n = 7$) or spontaneous PTL ($n = 7$). *$P < 0.05$; **$P < 0.01$, by 2-tailed *t*-test.

Nature Medicine: doi:10.1038/nm.4244

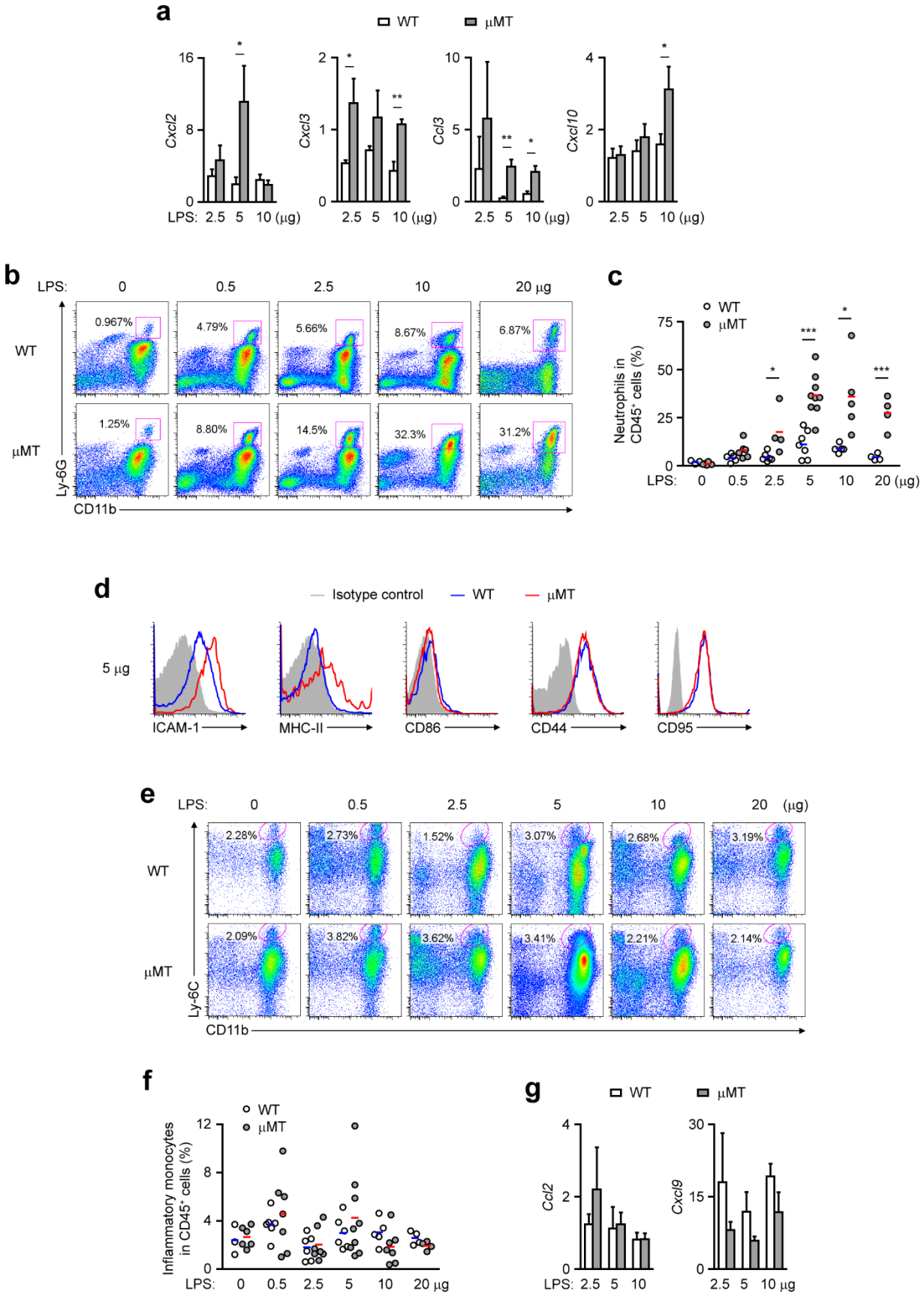

Nature Medicine: doi:10.1038/nm.4244

Supplementary Figure 4 B cell deficiency in mice causes heightened uterine inflammation and higher uterine neutrophil, but not inflammatory monocyte, infiltration and activation following LPS administration in late gestation. (**a**) Fold change of *Cxcl2*, *Cxcl3*, *Ccl3*, and *Cxcl10* transcripts in uterine tissues of gd 17.5 WT and μMT mice after receiving 2.5, 5 or 10 μg LPS, relative to the gene transcripts in uterine tissues of the respective mice that did not receive LPS. **P* < 0.05; ***P* < 0.01, by 2-tailed *t*-test. (**b**) Flow cytometric analysis of the frequency of $CD11b^+Ly\text{-}6G^+$ neutrophils in $CD45^+$ cells in uterine tissues of representative WT and μMT mice 24 hours after receiving LPS. (**c**) Statistical comparison of the frequencies of neutrophils in uterine $CD45^+$ leukocytes in WT and μMT mice after receiving LPS. **P* < 0.05; ****P* < 0.001, by 2-tailed *t*-test. (**d**) Expression of surface ICAM-1, MHC-II, CD86, CD44 and CD95 by viable neutrophils in uterine tissues of a representative WT or μMT mouse 24 hours after receiving 5 μg LPS. (**e**) Flow cytometric analysis of the frequency of $CD11b^+Ly\text{-}6C^+$ inflammatory monocyte in $CD45^+$ cells in uterine tissues of representative WT and μMT mice 24 hours after receiving LPS. (**f**) Statistical comparison of the frequencies of inflammatory monocytes in uterine $CD45^+$ leukocytes in WT and μMT mice after receiving LPS. (**g**) Fold change of *Ccl2* transcript in uterine tissues of gd 17.5 WT and μMT mice after receiving LPS, relative to the gene transcripts in uterine tissues of the respective mice that did not receive LPS. Data in **a** and **g** represent the results of 5 mice per group. Data in **b** and **c** represent the results of 3 WT mice (PBS group), 4 WT mice (20 μg LPS group), 5 WT mice (0.5 and 10 μg LPS groups), 6 WT mice (2.5 μg LPS group), 7 WT mice (5 μg LPS group), 4 μMT mice (2.5 and 20 μg LPS groups), 5 μMT mice (10 μg LPS group), 6 μMT mice (PBS and 0.5 μg LPS groups) or 9 μMT mice (5 μg LPS group) per group. Data in **d** represent the results of 7 WT mice and 9 μMT mice. Data in **e** and **f** represent the results of 3 WT mice (PBS group), 4 WT mice (20 μg LPS group), 5 WT mice (10 μg LPS group), 6 WT mice (0.5, 2.5 and 5 μg LPS groups), 4 μMT mice (20 μg LPS groups), 6 μMT mice (PBS group), 7 μMT mice (0.5, 2.5 and 10 μg LPS groups) or 9 μMT mice (5 μg LPS group) per group.

Nature Medicine: doi:10.1038/nm.4244

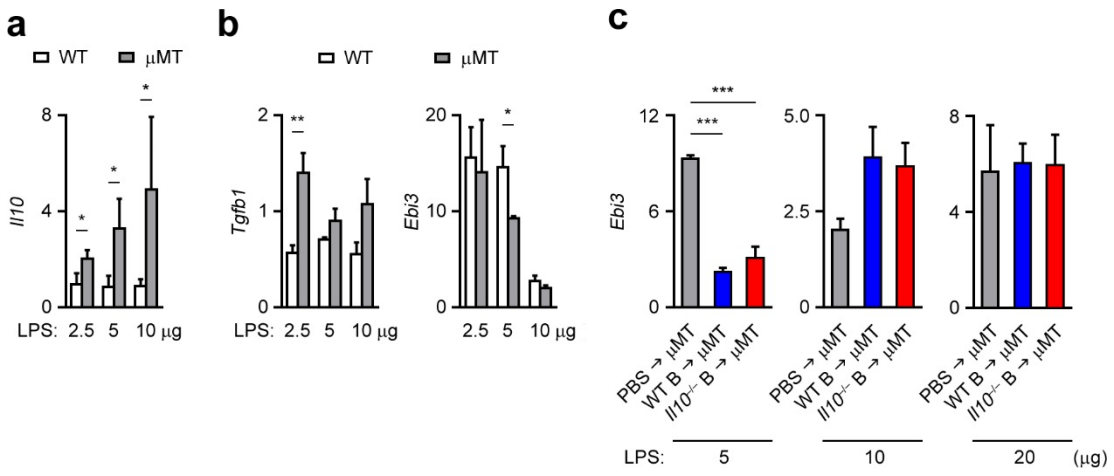

Supplementary Figure 5 B cells mediate protection against LPS-induced PTL in mice independently of IL-10, TGF-β or IL-35. (**a**,**b**) Fold change of *Il10*, *Tgfb1* and *Ebi3* transcripts in uterine tissues of gd 17.5 WT and μMT mice after receiving LPS, relative to the gene transcripts in uterine tissues of the respective mice that did not receive LPS. (**c**) Fold change of *Ebi3* transcript in uterine tissues of gd 17.5 μMT mice after receiving either PBS, or WT or *Il10*$^{-/-}$ B cells on gd 14.5 and LPS on gd 16.5, relative to the gene transcripts in uterine tissues of the respective mice that did not receive LPS. **P* < 0.05; ***P* < 0.01; ****P* < 0.001, by 2-tailed *t*-test. Data represent the results of 5 mice per group.

Nature Medicine: doi:10.1038/nm.4244

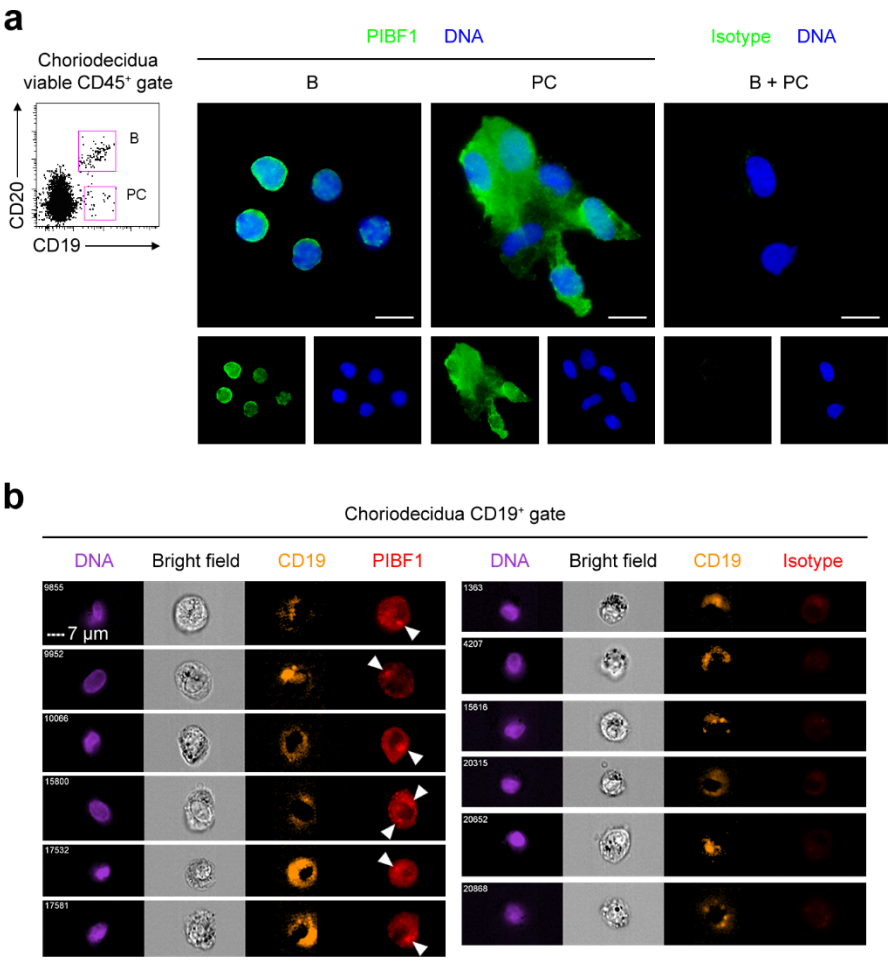

Supplementary Figure 6 Human choriodecidual B cells express PIBF1 at term delivery. (**a**) Cytospin followed by immunofluorescence analysis of PIBF1 expression by sorted $CD19^{+}CD20^{+}$ B cells and $CD19^{+}CD20^{-}$ PCs in choriodecidual tissue of a TL subject. Scale bars, 10 µm. (**b**) Imaging flow cytometry analysis of PIBF1 expression by TL choriodecidual $CD19^{+}$ B cells. Isotype control antibody-stained B cells were analyzed in parallel. Arrow heads point to concentrated perinuclear PIBF1 staining. Scale bar, 7 µm.

Nature Medicine: doi:10.1038/nm.4244

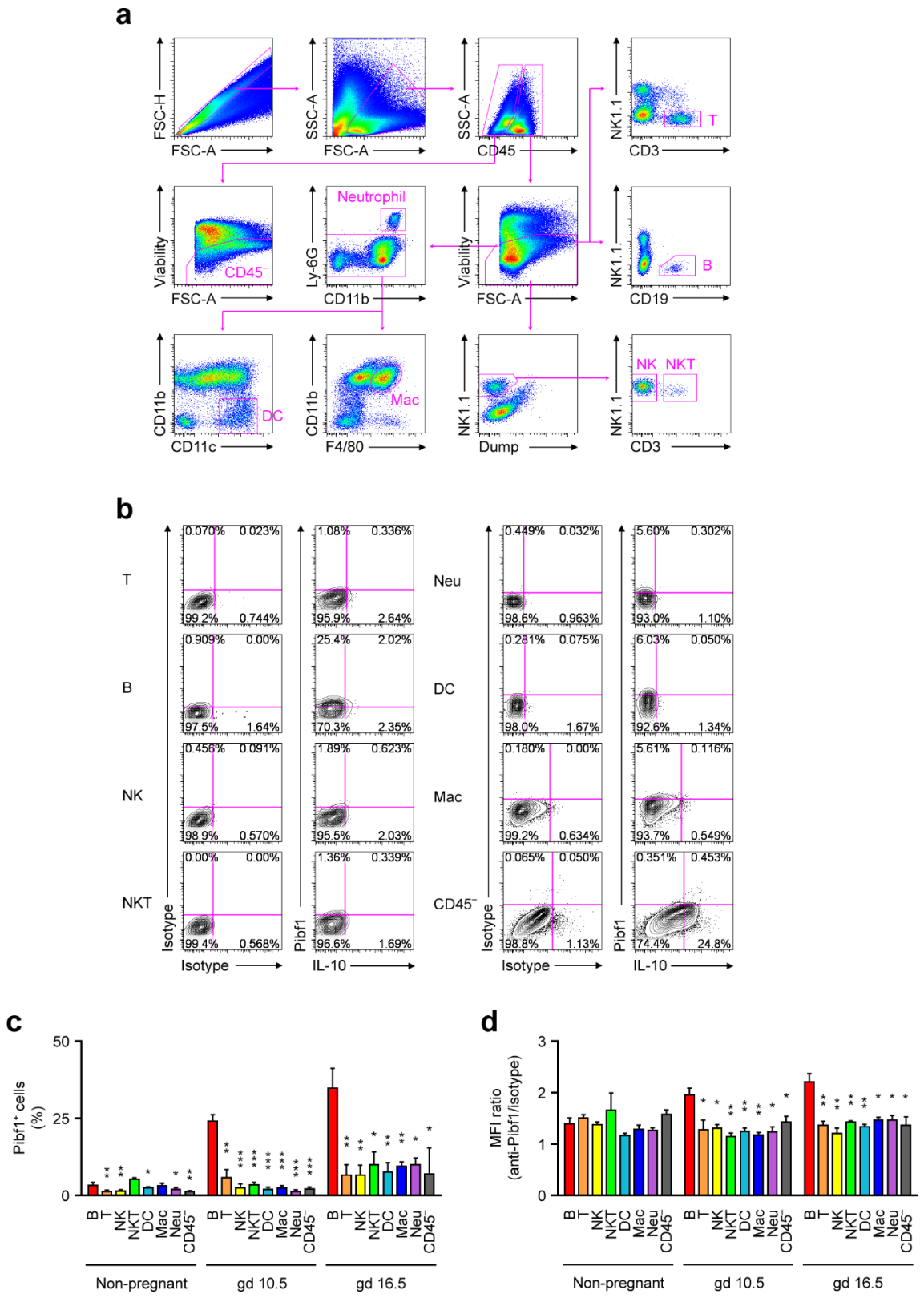

Supplementary Figure 7 B cells are a significant producer of Pibf1 in mouse uterus during late pregnancy. (**a**) The flow cytometric gating strategy for the identification of mouse uterine B

Nature Medicine: doi:10.1038/nm.4244

cells, T cells, NK cells, NKT cells, macrophages, DCs, neutrophils and $CD45^-$ resident cells. (**b**) Expression of Pibf1 and IL-10 by mouse uterine viable T cells, B cells, NK cells, NKT cells, neutrophils, DCs, macrophages and $CD45^-$ resident cells on gd 16.5. The quadrants were drawn based on the staining with isotype control antibodies. (**c**,**d**) Statistical comparisons of the frequencies of $Pibf1^+$ cells and ratios of mean fluorescence intensity (MFI) of Pibf1 to isotype control staining of the various uterine cell populations to that of B cells. $^*P < 0.05$; $^{**}P < 0.01$; $^{***}P < 0.001$, by 2-tailed *t*-test. Data represent the results from 4 WT C57BL/6 mice at each time point.

Nature Medicine: doi:10.1038/nm.4244

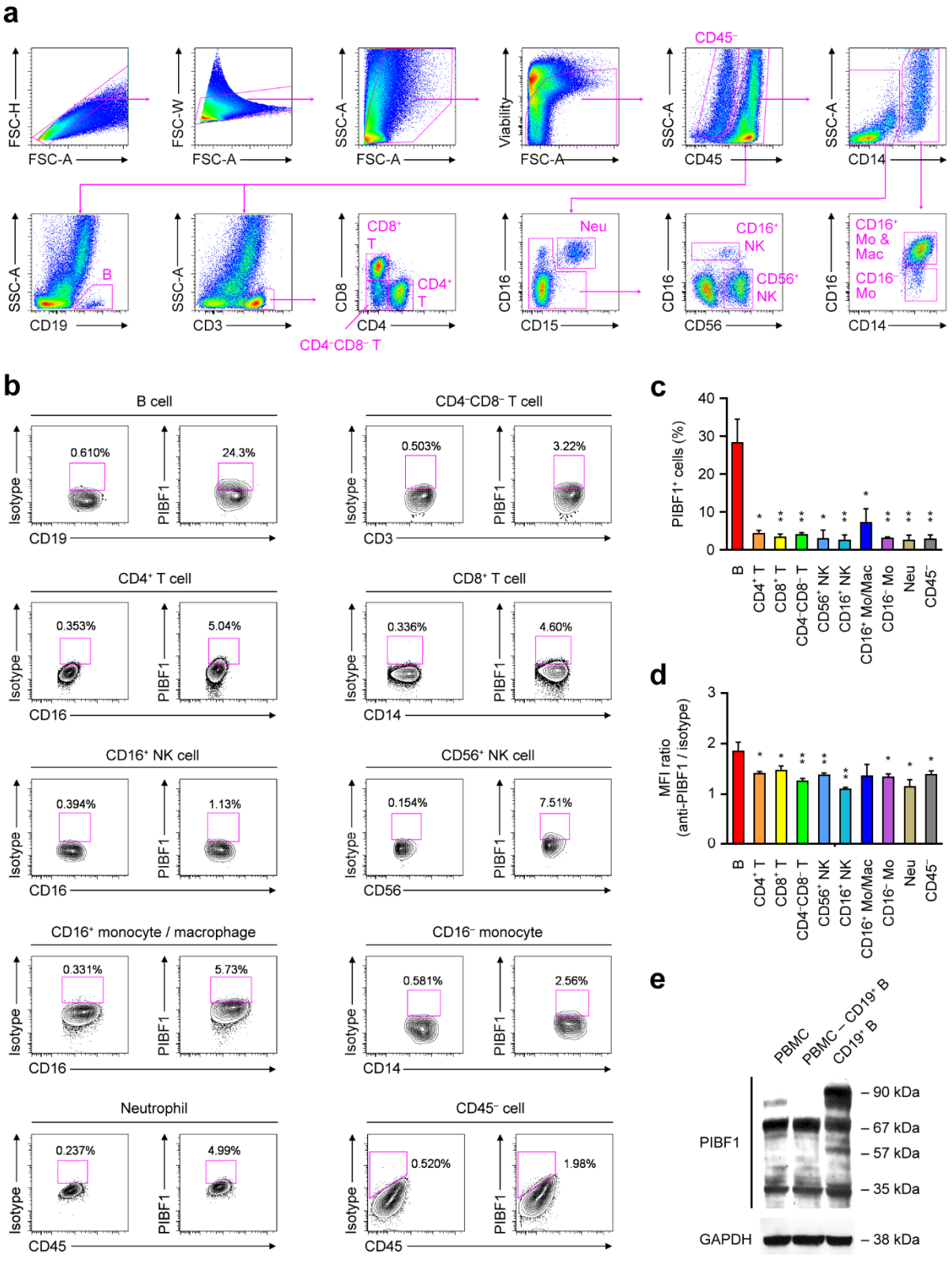

Supplementary Figure 8 B cells are a significant producer of PIBF1 in human choriodecidua at term delivery. (**a**) The flow cytometric gating strategy for the identification of human

Nature Medicine: doi:10.1038/nm.4244

choriodecidual B cells, $CD4^+$, $CD8^+$ and $CD4^-CD8^-$ T cells, $CD16^+$ and $CD56^+$ NK cells, $CD16^-$ monocytes and $CD16^+$ monocytes/macrophages, $CD15^+CD16^+$ neutrophils and $CD45^-$ resident non-hematopoietic cells. (**b**) Expression of PIBF1 by human choriodecidual viable B cells, $CD4^+$, $CD8^+$ and $CD4^-CD8^-$ T cells, $CD16^+$ and $CD56^+$ NK cells, $CD14^+CD16^-$ monocytes and $CD14^+CD16^+$ monocytes/macrophages, $CD15^+CD16^+$ neutrophils and $CD45^-$ resident non-hematopoietic cells at term delivery. The gates were drawn based on the staining with an isotype control antibody. (**c**,**d**) Statistical comparisons of the frequencies of $PIBF1^+$ cells and ratios of mean fluorescence intensity (MFI) of PIBF1 to isotype control staining of the various choriodecidual cell populations to that of B cells. $*P < 0.05$; $**P < 0.01$, by 2-tailed *t*-test. (**e**) Western Blot analysis ($n = 4$) of PIBF1 expression by PBMCs, PBMCs depleted of $CD19^+$ B cells and $CD19^+$ B cells of a representative healthy donor. Data in **c** and **d** represent the results of 5 subjects. Data in **e** represent the results of cells from 4 donors.

Nature Medicine: doi:10.1038/nm.4244

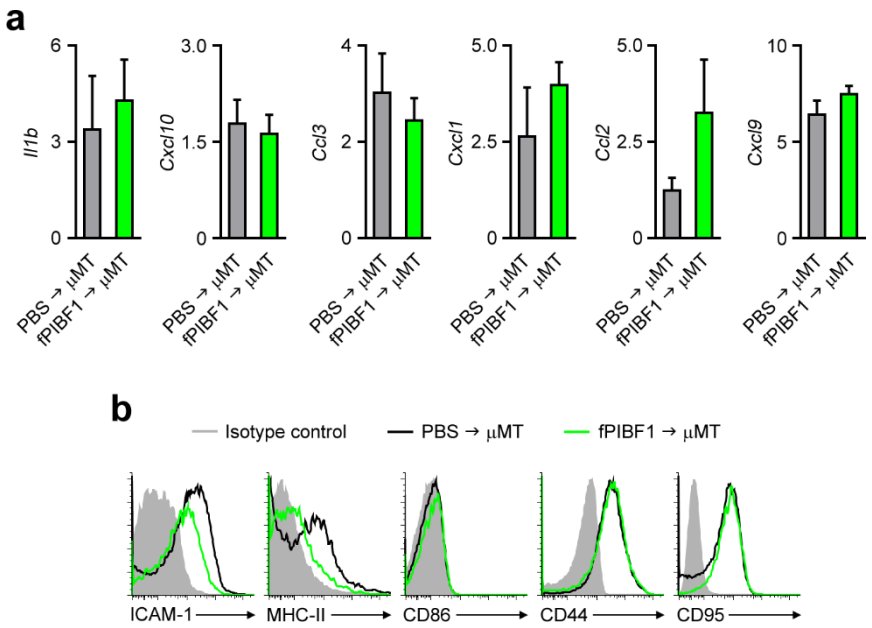

Supplementary Figure 9 Full-length PIBF1 administration suppresses uterine inflammation and neutrophil activation in LPS-challenged pregnant μMT mice. (**a**) Fold change of *Il1b*, *Cxcl10*, *Ccl3*, *Cxcl1*, *Ccl2* and *Cxcl9* transcripts in uterine tissues of gd 17.5 μMT mice after receiving 1 μg fPIBF1 and 5 μg LPS, relative to the gene transcripts in uterine tissues of the respective mice that received 1 μg fPIBF1 but not LPS. (**b**) Expression of surface ICAM-1, MHC-II, CD86, CD44 and CD95 by viable neutrophils in uterine tissues of a representative μMT mouse 24 hours after receiving PBS and 5 μg LPS (black histograms) or 1 μg fPIBF1 and 5 μg LPS (green histograms). Shaded histograms indicate the staining with isotype control antibodies. Data represent the results of 9 mice per group.

Nature Medicine: doi:10.1038/nm.4244

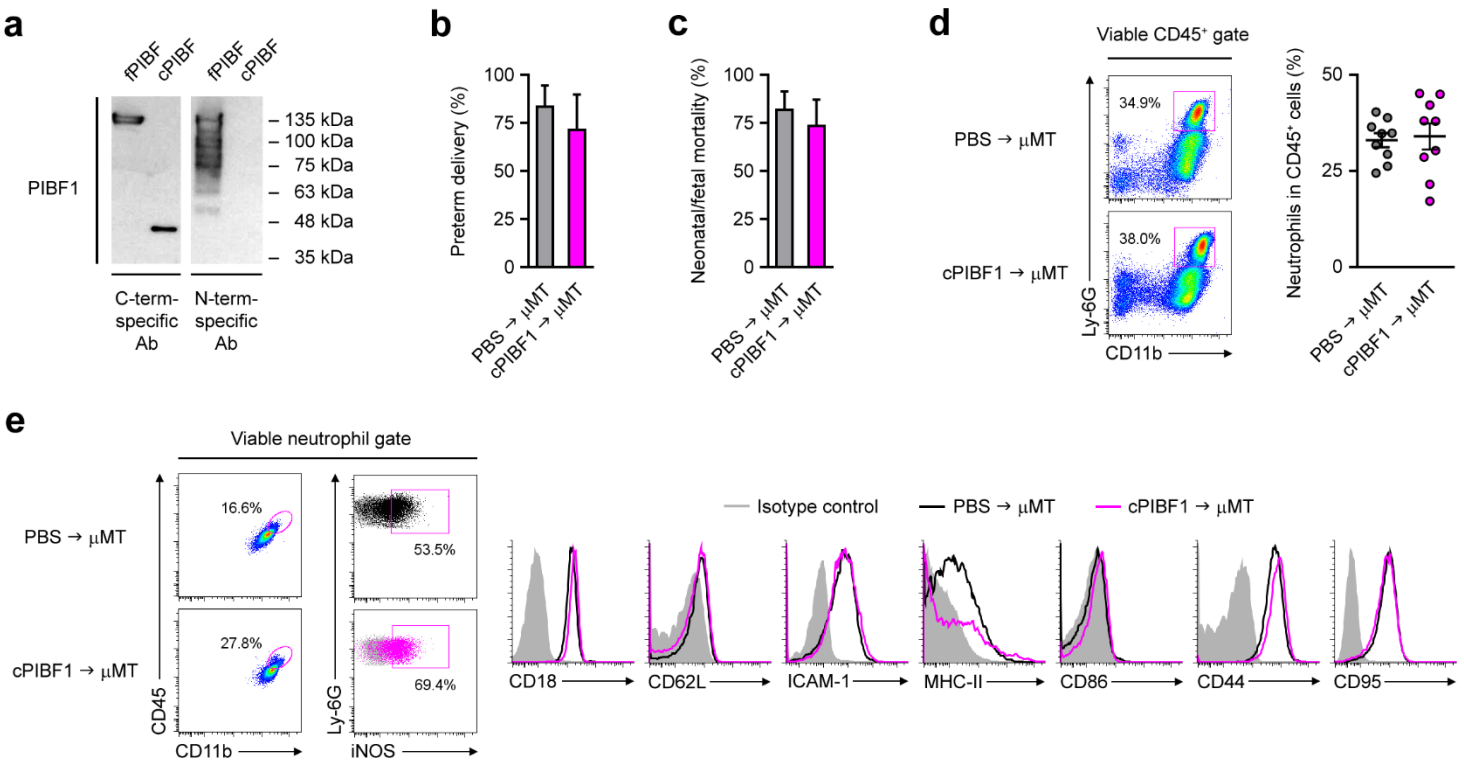

Supplementary Figure 10 A C-terminal fragment of PIBF1 does not protect μMT mice against LPS-induced PTL. (**a**) Western Blot analysis ($n = 2$) of fPIBF1 and cPIBF1 using a C-terminus-specific and an N-terminus-specific antibody. (**b**,**c**) Rates of preterm delivery and neonatal/fetal mortality on gd 17.5 of μMT mice that received either intravenous PBS or C-terminal fragment of PIBF1 (cPIBF1) and 5 μg intraperitoneal LPS on gd 16.5. (**d**,**e**) Frequency of $CD11b^{+}Ly\text{-}6G^{+}$ neutrophils in $CD45^{+}$ cells in uterine tissues of gd 17.5 μMT mice after receiving either intravenous PBS or C-terminal PIBF1 and intraperitoneal LPS on gd 16.5. (**f**) Expression of surface CD11b, CD18, CD62L, ICAM-1, MHC-II, CD86, CD44, CD95 and intracellular iNOS by viable neutrophils in uterine tissues of a μMT mouse 24 hours after receiving intravenous PBS or cPIBF1 and intraperitoneal LPS. Data represent the results from 9 mice per group. $*P < 0.05$; $**P < 0.01$; $***P < 0.001$, by Fisher's exact test (**a**), 1-tailed Mann–Whitney *U* test (**b**), or 1-tailed *t*-test (**d**).

Nature Medicine: doi:10.1038/nm.4244

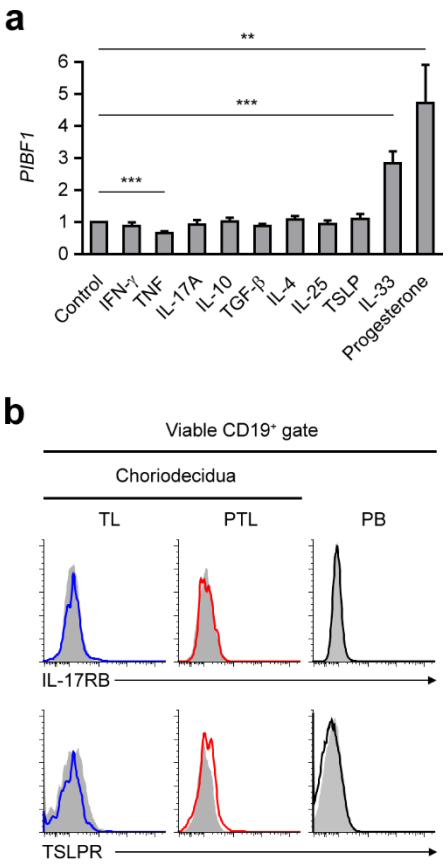

Supplementary Figure 11 IFN-γ, TNF, IL-17A, IL-4, IL-10, TGF-β, IL-25 and TSLP do not induce PIBF1 expression by human B cells. (**a**) Fold change of *PIBF1* transcript in purified human peripheral blood IgD^+ B cells after 2 days of treatment with medium (control), IFN-γ, TNF, IL-17A, IL-4 or IL-10, TGF-β, IL-25, TSLP, IL-33 or progesterone. $^{**}P < 0.01$; $^{***}P < 0.001$, by 2-tailed *t*-test. (**b**) Flow cytometric analysis of the expression of the IL-25 receptor subunit IL-17RB and TSLP receptor (TSLPR) on peripheral blood, TL and PTL choriodecidual B cells. Data in **a** are representative of 3 independent experiments. Data in **b** represent the results of 10 blood donors, 10 women with TL and 10 women with PTL.

Nature Medicine: doi:10.1038/nm.4244

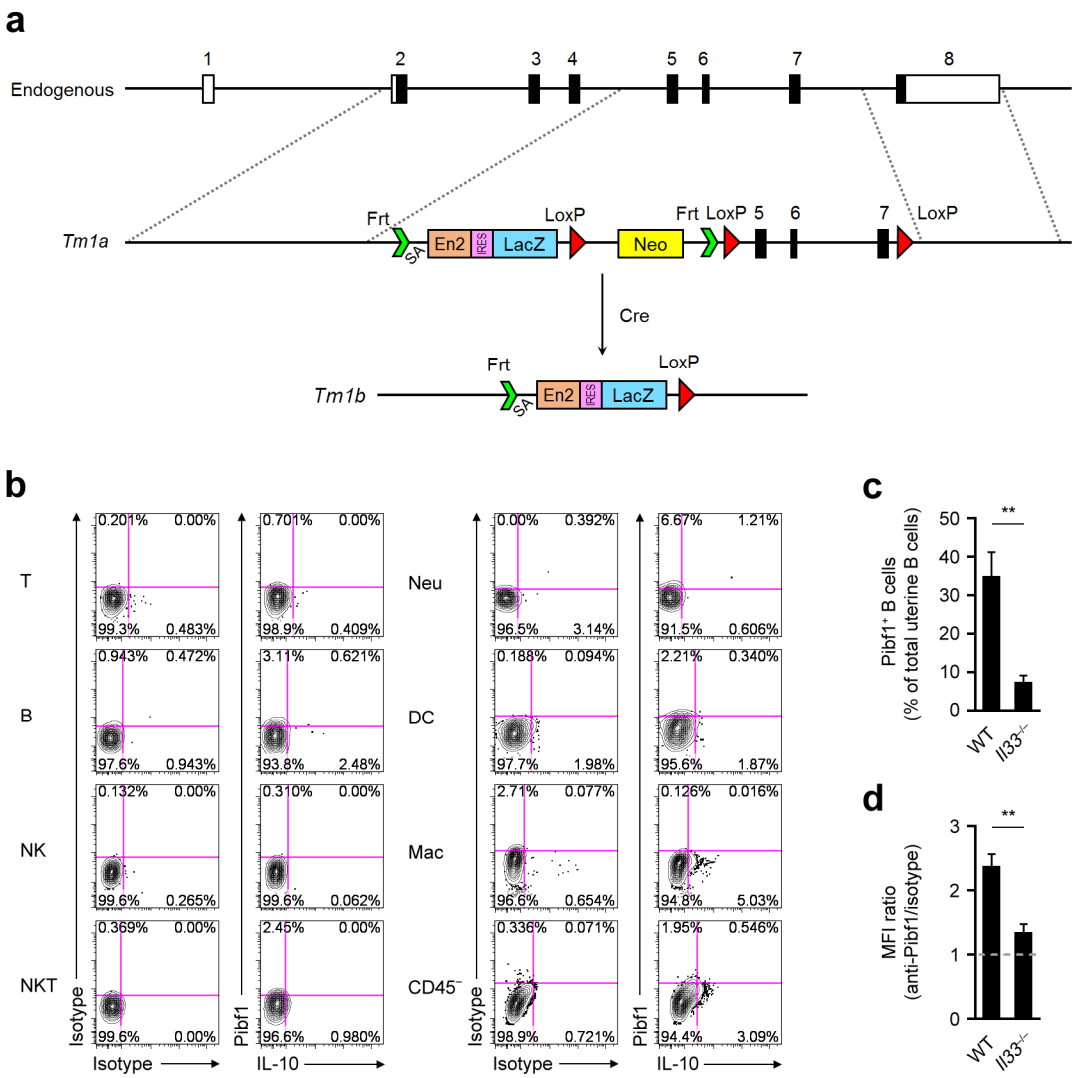

Supplementary Figure 12 Pibf1 expression is diminished in uterine tissues and uterine B cells in *Il33*$^{-/-}$ mice. (**a**) Schematic representation of the disruption of the *Il33* locus in the *Il33*$^{-/-}$ *lacZ* reporter mouse. The targeting vector *Il33*^{Tm1a} contains an En2/IRES/LacZ/Neo/pA cassette preceding exons 5–7 of the *Il33* gene that are flanked by LoxP sites. This targeting vector was introduced into the C57BL/6 mouse ES cell line B6-13. The *Il33*^{tm1b} allele was generated by breeding *Il33*^{tm1a} mice with CMV-*Cre* transgenic mice of the C57BL/6 background, resulting in the deletion of exons 5–7 and the Neo cassette. The *Cre* transgene was subsequently bred out. SA: splicing acceptor. Open boxes represent untranslated regions in mouse *Il33* mRNA. (**b**) Flow cytometry of Pibf1 expression in uterine cells of a pregnant *Il33*$^{-/-}$ mice on gd 16.5. (**c**,**d**) Statistical comparisons of the frequencies of Pibf1^{+} uterine B cells and ratios of MFI of Pibf1 to isotype control staining of uterine B cells of pregnant WT and *Il33*$^{-/-}$ mice on gd 16.5. $^{**}P < 0.01$, by 2-tailed *t*-test. Data represent the results of 3 mice in each group.

Nature Medicine: doi:10.1038/nm.4244

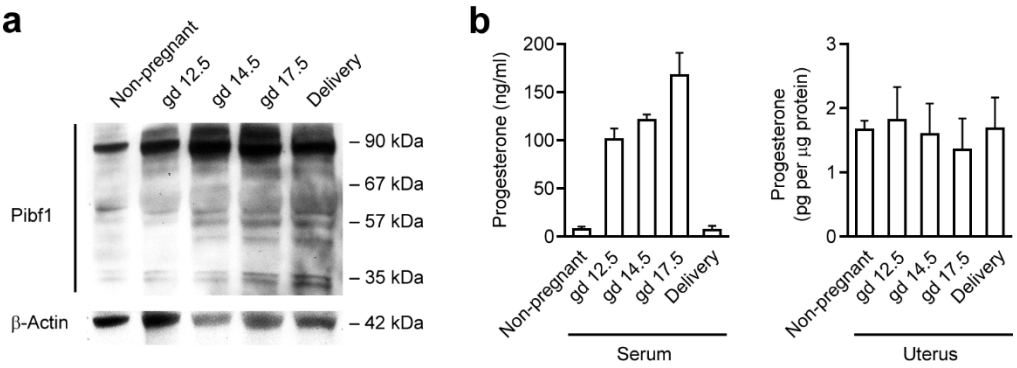

Supplementary Figure 13 Mouse uterine Pibf1 expression does not reduce amidst systemic progesterone withdrawal in late gestation. (**a**) Western Blot analysis ($n = 2$) of Pibf1 expression in non-pregnant mouse uterus and the uterus of pregnant mice on gd 12.5, 14.5, 17.5 or immediately after delivery. (**b**) ELISA of serum progesterone concentration at the corresponding time point. The result represents 3 mice per time point.

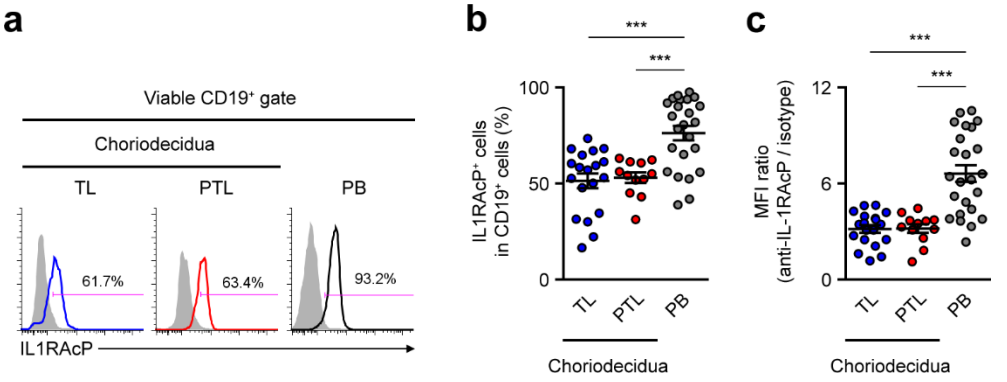

Supplementary Figure 14 Peripheral blood and choriodecidual B cells constitutively express IL1RAcP. (**a**) Flow cytometric analysis of the expression of IL1RAcP on peripheral blood, TL and PTL choriodecidual B cells. Shaded histograms indicate the staining with an isotype control antibody. (**b**,**c**) Statistical comparison of the frequencies of IL1RAcP$^+$ B cells and the ratios of MFI of IL1RAcP to isotype control staining of B cells in peripheral blood (n = 24), TL choriodecidua ($n = 19$) and PTL choriodecidua ($n = 12$). ***$P < 0.001$, by 2-tailed Mann–Whitney U test (for Term vs. PB and Preterm vs. PB in b) or 2-tailed t-test (all other comparisons).

Nature Medicine: doi:10.1038/nm.4244

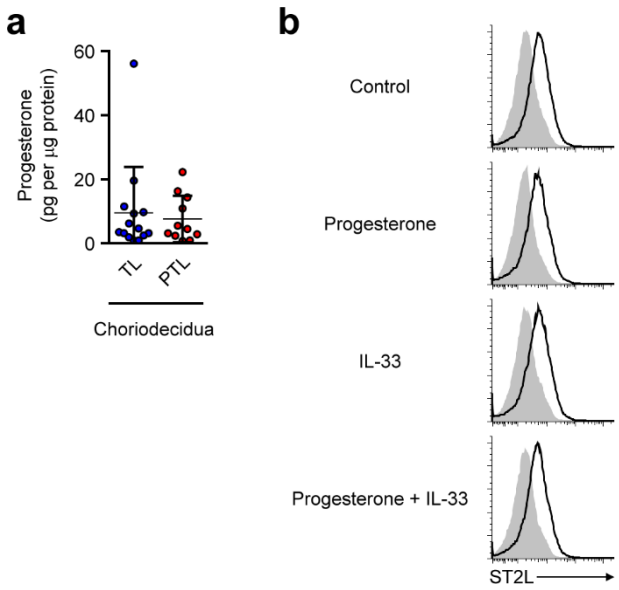

Supplementary Figure 15 Diminished ST2L expression on human PTL choriodecidual B cells was not due to lower choriodecidual progesterone. (**a**) ELISA of progesterone levels in choriodecidual tissues of TL (n = 14) and PTL (n = 11) subjects at delivery, normalized to per µg of choriodecidual protein. (**b**) Flow cytometric analysis of ST2L expression by human PB IgD^+ B cells treated for 3 days with medium (Control), progesterone, IL-33, or progesterone and IL-33. Shaded histograms indicate the staining with an isotype control antibody. Results represent the B cells of 3 donors.

Nature Medicine: doi:10.1038/nm.4244

Full-length blots

Fig. 3a

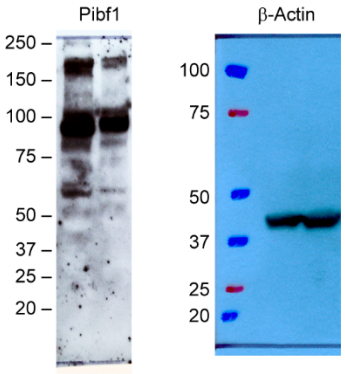

Fig. 3e

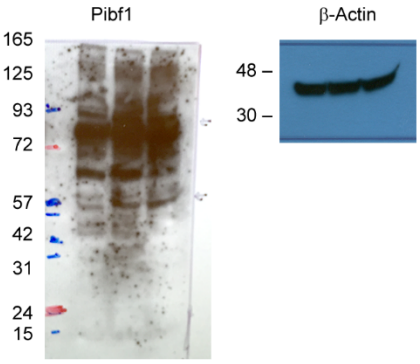

Fig. 4b

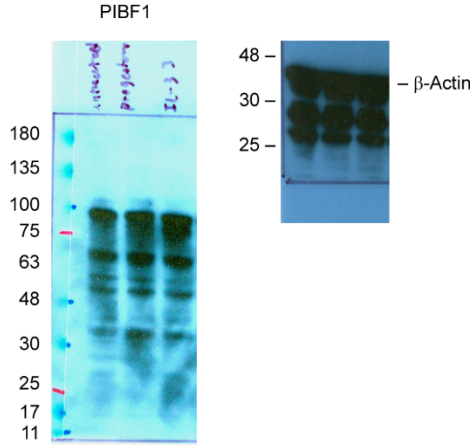

Fig. 4c

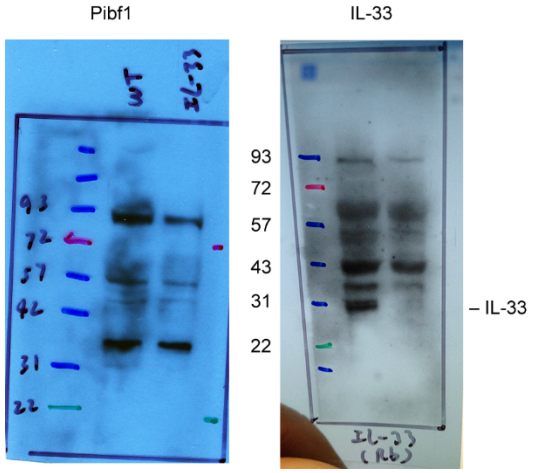

Fig. 4h

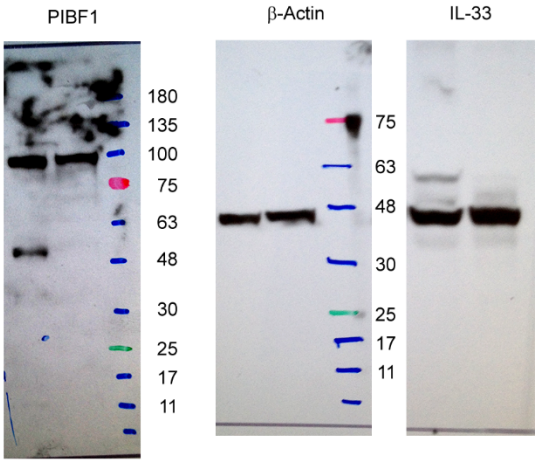

Nature Medicine: doi:10.1038/nm.4244

Fig. S8e

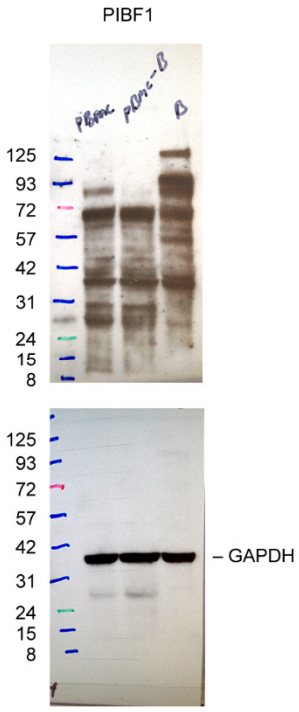

Fig. S10a

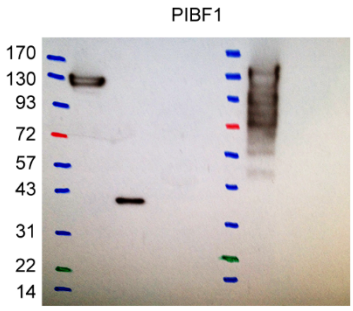

Fig. S13a

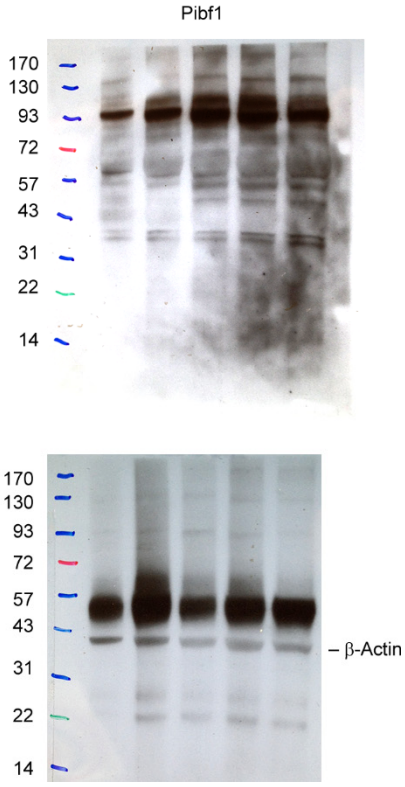

Nature Medicine: doi:10.1038/nm.4244